Cells lacking the fumarase tumor suppressor are protected from apoptosis through a hypoxia-inducible factor-independent, AMPK-dependent mechanism

Cells Lacking the Fumarase Tumor Suppressor Are Protected from Apoptosis through a Hypoxia-Inducible Factor-Independent, AMPK-Dependent Mechanism

Chiara Bardella, Martina Olivero, Annalisa Lorenzato, Massimo Geuna, Julie Adam, Linda O'Flaherty, Pierre Rustin, Ian Tomlinson, Patrick J. Pollard and Maria Flavia Di Renzo

Mol. Cell. Biol. **2012, 32(15):3081. DOI: 10.1128/MCB.06160-11.**
Published Ahead of Print 29 May 2012.

MCB
Journals.ASM.org

Cells Lacking the Fumarase Tumor Suppressor Are Protected from Apoptosis through a Hypoxia-Inducible Factor-Independent, AMPK-Dependent Mechanism

Chiara Bardella,[a,b]* Martina Olivero,[a,b] Annalisa Lorenzato,[a,b] Massimo Geuna,[c] Julie Adam,[d] Linda O'Flaherty,[d] Pierre Rustin,[e,f] Ian Tomlinson,[g] Patrick J. Pollard,[d] and Maria Flavia Di Renzo[a,b]

Department of Oncological Sciences, University of Torino, School of Medicine, Turin, Italy[a]; Laboratory of Cancer Genetics, Institute for Cancer Research at Candiolo (IRCC), Candiolo, Turin, Italy[b]; Laboratory of Immunopathology, Department of Pathology, ASO Ordine Mauriziano, Turin, Italy[c]; Henry Wellcome Building for Molecular Physiology, University of Oxford, Oxford, United Kingdom[d]; INSERM, U676, Paris, France[e]; Université Paris 7, Faculté de Médecine Denis Diderot, IFR02, Paris, France[f]; and Molecular and Population Genetics Laboratory and Oxford NIHR Comprehensive Biomedical Research Centre, Wellcome Trust Centre for Human Genetics, University of Oxford, Oxford, United Kingdom[g]

Loss-of-function mutations of the tumor suppressor gene encoding fumarase (*FH*) occur in individuals with hereditary leiomyomatosis and renal cell cancer syndrome (HLRCC). We found that loss of FH activity conferred protection from apoptosis in normal human renal cells and fibroblasts. In FH-defective cells, both hypoxia-inducible factor 1α (HIF-1α) and HIF-2α accumulated, but they were not required for apoptosis protection. Conversely, AMP-activated protein kinase (AMPK) was activated and required, as evidenced by the finding that FH inactivation failed to protect AMPK-null mouse embryo fibroblasts (MEFs) and AMPK-depleted human renal cells. Activated AMPK was detected in renal cysts, which occur in mice with kidney-targeted deletion of *Fh1* and in kidney cancers of HLRCC patients. In *Fh1*-null MEFs, AMPK activation was sustained by fumarate accumulation and not by defective energy metabolism. Addition of fumarate and succinate to kidney cells led to extracellular signal-regulated kinase 1/2 (ERK1/2) and AMPK activation, probably through a receptor-mediated mechanism. These findings reveal a new mechanism of tumorigenesis due to FH loss and an unexpected pro-oncogenic role for AMPK that is important in considering AMPK reactivation as a therapeutic strategy against cancer.

The fumarase gene (*FH*; fumarate hydratase gene) encodes a highly conserved protein (EC 4.2.1.2) which in mitochondria catalyzes the conversion of fumarate to malate as part of the tricarboxylic acid cycle (TCA or Krebs cycle). Germ line mutations in *FH* are associated with two distinct diseases. In the homozygous or compound heterozygous state, biallelic *FH* mutations cause an autosomal recessive disease, the fumarase deficiency syndrome (also known as fumaric aciduria; OMIM accession no. 606812), characterized by severe impairment in the development of the central nervous system (CNS) (2). Heterozygous germ line mutations predispose individuals to multiple smooth muscle tumors of the skin and uterus (multiple cutaneous and uterine leiomyomatosis [MCUL]; OMIM accession no. 150800) and to an increased risk of papillary renal carcinoma and leiomyosarcoma (hereditary leiomyomatosis and renal cell cancer syndrome [HLRCC]; OMIM accession no. 605839) (56). The high frequency of inactivation of the second allele and loss of enzymatic activity in tumor cells indicate that *FH* is a tumor suppressor gene (56).

Loss of FH activity triggers pseudohypoxic signaling (14). Accumulation of fumarate and succinate results in the inhibition of the prolyl-hydroxylases (PHDs) (42, 51), which physiologically hydroxylate the HIF-α subunits of the hypoxia-inducible transcription factor (HIF) when oxygen is available (8). HIF is a heterodimer composed of the labile HIF-α and stable HIF-β/ARNT (aryl hydrocarbon receptor nuclear translocator) subunits (52), which form a transcriptionally active complex in the nucleus. The best-known function of HIF is to promote adaptation of cells to hypoxia (37). In leiomyomas and renal tumors of HLRCC patients, high levels of intracellular fumarate accumulate, HIF-α subunits are stabilized, and HIF target genes are transcribed in ambient normoxia, mimicking hypoxic conditions (pseudohypoxia) (23, 42). There is strong evidence to suggest that fumarate-mediated inhibition of PHD activity and subsequent HIF accumulation and activation are direct consequences of FH loss and the cause of the observed pseudohypoxia (19, 39). Further evidence has come from the conditional inactivation of mouse *Fh1* in the kidney, which leads to the development of multiple clonal renal cysts that overexpress Hif-1α, Hif-2α, and Hif target genes such as *Glut1* and *Vegf* (44). These and other HIF target genes promote the glycolytic and angiogenic shifts that favor tumor progression. However, although several studies have demonstrated upregulation of HIF in FH-associated neoplasia, this does not prove that HIF accumulation is the causative oncogenic mechanism.

How somatic cells survive with a Krebs cycle defect has been explained, although a loss of FH activity is lethal for human developing neurons carrying homozygous germ line mutations in the FH gene (2). Indeed, it has been proposed that somatic cells with

Received 22 August 2011 **Returned for modification** 17 October 2011
Accepted 19 May 2012

Published ahead of print 29 May 2012

Address correspondence to Maria Flavia Di Renzo, mariaflavia.direnzo@unito.it.

* Present address: Chiara Bardella, Molecular and Population Genetics Laboratory, Wellcome Trust Centre for Human Genetics, University of Oxford, Oxford, United Kingdom.

doi:10.1128/MCB.06160-11

FH loss surmount energetic impairment by becoming glucose addicted (55, 58) or using glutamine as a major source of energy (7). More recently, it was shown that the glutamine uptake in *Fh1*-deficient cells enables the use of accumulated TCA cycle metabolites and permits partial mitochondrial production of NADH, given that biosynthesis and degradation of heme are activated (11). However, this can explain how cells tolerate the Krebs cycle defect but not how they overcome the apoptotic signaling triggered by the stresses that cancer cells experience during the course of tumorigenesis (35). Here we show not only that FH-defective cells can survive but also that they exhibit increased resistance to apoptosis induced by different stimuli. Furthermore, we demonstrate that apoptosis protection is mediated predominantly by the activation of the AMP-activated protein kinase (AMPK).

MATERIALS AND METHODS

Chemicals, antibodies, and cell lines. Cisplatin (CDDP) was obtained from Bristol-Myers Squibb (Rocky Hill, NJ). Staurosporine, AICAR (5-aminoimidazole-4-carboxamide-1-β-4-ribofuranoside), *N*-acetyl-L-cysteine, sodium pyruvate, sodium oxamate, succinate, diethyl succinate, and monoethyl fumarate were obtained from Sigma (Steinheim, Germany). Metformin was obtained from MP Biomedicals (Illkirsch, France). A-769662 was obtained from Tocris Bioscience (Bristol, United Kingdom), and cobalt chloride was purchased from Fluka BioChemika (Buchs, Switzerland). Rabbit polyclonal anti-FH antibody was obtained from Nordic Immunological Laboratories (Tilburg, The Netherlands). Anti-human and -mouse HIF-1α and anti-HIF-2α polyclonal antibodies were obtained from Novus Biologicals (Littleton, CO). The anti-glyceraldehyde-3-phosphate dehydrogenase (anti-GAPDH) mouse monoclonal antibody (MAb) 6C5 was obtained from Ambion (Foster City, CA). Anti-human vinculin MAb and anti-human tubulin MAb were obtained from Sigma-Aldrich. Anti-BAD, anti-phosphorylated protein kinase A (anti-P-PKA) (Thr197), anti-PKA, anti-P-p70S6K (Thr421/Ser424), anti-p70S6K, anti-P-p38 mitogen-activated protein kinase (MAPK) (Thr180/Tyr182), anti-p38 MAPK, anti-P-AKT (Ser473), anti-AKT, anti-P-AMPK (Thr172), anti-AMPK, anti-MCL-1, anti-BCL-X_L, anti-BMF, anti-BAX, anti-BCL-2, anti-P-BCL-2 (Ser70), anti-P-Erk1/2 (Thr202/Tyr204), anti-Erk1/2, and anti-P-ACC (Ser 79) rabbit polyclonal antibodies, anti-acetyl coenzyme A carboxylase (anti-ACC) rabbit monoclonal antibody, and anti-P-BAD (Ser112) mouse monoclonal antibody were all obtained from Cell Signaling Technology (Beverly, MA). Anti-V5 antibody was obtained from Invitrogen (Eugene, OR). FH-negative fibroblasts were derived from skin biopsy specimens from a patient suffering from fumaric aciduria and homozygous for a missense mutation (2). Control fibroblasts were propagated from a skin biopsy specimen from a healthy individual. Renal proximal tubule epithelial cells (RPTEC), HK-2 cells, and Hepa-1c1c7 cells and their mutant derivative c4 and vT{2} clones were purchased from the American Type Culture Collection (Manassas, VA) and grown as suggested by the provider. Simian virus 40 (SV40)-immortalized AMPK α1/α2 double-knockout mouse embryo fibroblasts (MEFs) and relevant control SV40-immortalized mouse fibroblasts were obtained from Benoit Viollet (29). Immortalized Fh1-deficient MEFs were generated and propagated as described elsewhere (39). To investigate the effects of low and high levels of glucose supplementation of the culture medium, Dulbecco's modified Eagle's medium (DMEM) without glucose was supplemented with D-(+)-glucose from Sigma (Sigma-Aldrich, France).

Human and murine tissues. FH mutant type II papillary renal cancers from paraffin-embedded sections were collected with full ethical approval, in collaboration with Ian Tomlinson (Oxfordshire Research Ethics Committee [REC] B approval 05/Q1605/66 [Molecular Analyses of Archival Tumors for Human Tissues]). FH-deficient renal cysts and cells were derived from FH mutant mice. All procedures were carried out in accordance with Home Office UK regulations and the Animals (Scientific Procedures) Act 1986. Fh1-deficient mice have been described elsewhere (44).

Cell transduction with lentiviral vectors (LV). An FH-specific short hairpin RNA (shRNA) sequence (forward sequence, 5′-GGAAUUUA GUGGUUAUGUU-3′) was cloned into the pSUPER vector. Lentiviral shRNAs were generated by subcloning the H1-RNA-promoter-shRNA cassette from pSUPER into EcoRI-HindIII sites of the vector pCCL.sin. PPT.hPGK.GFP.Wpre.

As a control, cells were also transduced with a scrambled shRNA (forward sequence, 5′-AGUCUACAUGCUCACACUU-3′) sequence cloned into the vector pCCL.sin.PPT.hPGK.GFP.Wpre, under the control of the H1-RNA-promoter sequence. For FH rescue, an RNA interference-resistant *FH* cDNA was obtained by insertion of 8 different silent mutations, specific for the shRNA used, into the *FH* cDNA sequence. All mutations were introduced using a PCR-based technique as described elsewhere (34). Briefly, human FH cDNA, previously subcloned as a BamHI-SalI fragment into the transfer vector pRRL.sin.PPT.hCMV.pre, was amplified by a PCR protocol including two different courses of amplification. Subsequently, the FH mutant cDNA cassette, subcloned into the pDRIVE vector, was cloned into the lentiviral pRRL.sin.PPT.hCMV.hFH.pre transfer vector as an XbaI-PstI fragment. The PCR primer set used to introduce the silent mutations into the FH cDNA and the PCR amplification conditions used are available upon request. The following HIF-1α-specific shRNAs were obtained from the Open Biosystem TRC lentiviral shRNA library: RHS3979-9572497 and RHS3979-9572499. The following AMPK-α1- and -α2-specific shRNAs were obtained from the Sigma-Aldrich TRC lentiviral shRNA library: SHCLNG-NM_006251 (5 clones) and SHCLNG-NM_006252 (5 clones). The pLL3.7 lentiviral vectors containing either BAD-specific or control shRNAs were kindly provided by G. Kulik (Department of Cancer Biology, Wake Forest University School of Medicine, Winston-Salem, NC). Vector stocks were produced by transient transfection of 293T cells. Serial dilutions of freshly harvested conditioned medium were used to infect 10^5 cells in a six-well plate, in the presence of Polybrene (8 μg/ml). The viral p24 antigen concentration was measured by an HIV-1 p24 core profile enzyme-linked immunosorbent assay (ELISA; NEN Life Science Products) to determine the number of infective particles before transduction and to demonstrate that transduced cells did not produce viral particles after transduction.

Measurement of ROS production. The fluorogenic dye MitoSOX Red (Molecular Probes, Invitrogen Detection Technologies), a mitochondrial superoxide indicator, was used to detect reactive oxygen species (ROS) in the mitochondria of live cells, following the instructions of the manufacturer. Briefly, 3×10^5 HK-2 cells were plated in 6-well plates, and after 24 h, they were either left untreated or treated with hydrogen peroxide at the indicated concentration for 2 h and then incubated with 0.5 μM MitoSOX solution for 20 min at 37°C, protected from light. After washing with phosphate-buffered saline (PBS), cells were harvested with trypsin, resuspended in a suitable buffer, and analyzed with a flow cytometer.

Flow cytometry analysis of apoptosis induction. Apoptosis was measured by staining with allophycocyanin (APC)-conjugated annexin V (Bender MedSystems, Burlingame, CA) and propidium iodide (Invitrogen, Eugene, OR), which allow detection of the phosphatidylserine (PS) exposure on the cell surface and the loss of plasma membrane integrity, respectively. Cell viability was measured as the percentage of propidium iodide-negative cells. To evaluate the effects of antioxidants and a lactate dehydrogenase (LDH) inhibitor on apoptosis induction, cells were treated with *N*-acetylcysteine, sodium pyruvate, or sodium oxamate together with cisplatin at the indicated concentrations. Caspase activation was determined with anti-active caspase-3 (BD PharMingen, San Diego, CA) as the primary antibody and a phycoerythrin (PE)-conjugated goat anti-rabbit antibody (BD PharMingen, San Diego, CA) as the secondary antibody. Samples were analyzed on a FACSCalibur flow cytometer (Bec-

ton, Dickinson, San Diego, CA). Data acquisition was performed using CellQuest software (Becton, Dickinson, San Diego, CA).

Quantitative reverse transcription-PCR. Total RNA was extracted and purified using an RNA purification reagent (Promega, Madison, WI) following the manufacturer's instructions. RNAs were then quantified and inspected by Bioanalyzer (Agilent Technologies, Waldbrom, Germany) analysis. cDNA was synthesized from 1 μg RNA by use of Moloney murine leukemia virus reverse transcriptase H^- [MMLV-RT(H−)] enzyme (Promega, Madison, WI). Quantitative real-time PCR was done on an MyiQ thermal cycler (Bio-Rad, Hercules, CA); all quantitative PCR mixtures contained 40 ng retrotranscribed RNA, 1× SYBR green PCR master mix (2× stock; Applera, Foster City, CA), and 300 μM (each) target-specific primers. Each target gene's expression was evaluated using a relative quantification approach ($2^{-\Delta\Delta CT}$ method), with cyclophilin A (PPIA; GenBank accession no. NM_021130) as an internal reference. Primer sets and PCR cycling conditions are available upon request.

Protein extraction and Western blot analysis. For nuclear protein analysis, cells were incubated at 4°C for 10 min with 1 ml of buffer A, containing 10 mM HEPES, pH 7.9, 10 mM KCl, 10 mM EDTA, 1 mM dithiothreitol (DTT), 0.5% NP-40, and phosphatase and protease inhibitors (2 mM sodium orthovanadate, 1 μg/ml leupeptin, 1 μM pepstatin, 1 mM phenylmethylsulfonyl fluoride, 100 μg/ml soybean trypsin inhibitor). Cell extracts were then centrifuged at 15,000 × *g* for 3 min, and the supernatant (cytosolic) fraction was collected. The pellet was resuspended in 150 μl of buffer B (20 mM HEPES, pH 7.9; 0.4 M NaCl; 1 mM EDTA; 50% glycerol; 1 mM DTT; and the phosphatase and protease inhibitors described above) and incubated on a rocking platform at 200 rpm for 2 h at 4°C. After centrifugation at 15,000 × *g* for 5 min, the supernatant was collected as the nuclear fraction. For PAGE gels, SDS-containing buffer was added to the fractions. Total protein extraction was performed by directly incubating cells in SDS-containing lysis buffer at 95°C for 5 min. Proteins were separated by PAGE and transferred to nitrocellulose sheets. Equal amounts of proteins (100 μg) were loaded in each lane. Blots were probed and, when necessary, reprobed with different antibodies as indicated in Results. Bound antibodies were detected using the appropriate peroxidase-conjugated secondary antibody and revealed by enhanced chemiluminescence (Pierce, Rockford, IL).

Quantitative phosphoprotein assays. Phosphorylation of kinases and kinase substrates was measured using a Bio-Plex phosphoprotein assay (Bioclarma, Turin, Italy) according to the manufacturer's protocol. Lysates were prepared, and phosphorylated proteins were detected with a Bio-Rad phosphoprotein immunoassay kit, using a Bio-Plex 100 system and workstation according to the manufacturer's protocol. Data acquisition and analysis were done using Bio-Plex Manager software, version 4.1.1, according to the manufacturer's instructions. In the assay, antibodies to the following phosphorylated proteins were used: P-p90RSK (Thr359, Ser363), P-c-Jun (Ser63), phosphorylated glycogen synthase kinase 3a/b (P-GSK-3a/b) (Ser9, Ser21), P-ATF-2 (Thr71), P-MEK1 (Ser217, Ser221), phosphorylated extracellular signal-regulated kinase 1/2 (P-ERK1/2) (Thr202, Tyr204, Thr185, Tyr187), and phosphorylated Jun N-terminal kinase (P-JNK) (Thr183, Tyr185). Protein phosphorylation was investigated further using Western blot analysis with the antibodies listed above. AMPK phosphorylation was quantified using a PathScan phospho-AMPKα ELISA kit (Cell Signaling Technology, Beverly, MA) following the manufacturer's instructions.

Measurement of FH enzymatic activity. FH enzyme measurement was performed on HK-2 cell pellets. Cells/organelles were disrupted by freeze-thawing. Fumarase activity was measured spectrophotometrically according to standard procedures. Briefly, the assay monitors the increase in absorbance at 250 nm due to conversion of malate to fumarate in a reaction medium containing 10 mM KH_2PO_4, pH 7.8, 2 mM EDTA, 50 mM malate, and 0.1% Triton X-100. Enzyme activity was measured at 37°C. Protein concentration was determined by the Bradford assay. Reagents were of the highest grade commercially available from Sigma-Aldrich (France).

Measurement of ADP:ATP ratio. The ADP:ATP ratio was determined by a luminometric method, using an ApoSENSOR ratio assay kit (BioVision, Mountain View, CA) according to the manufacturer's instructions. The background-subtracted luminescence values (relative light units) were normalized to the total protein in each sample. The results of five independent experiments are reported.

Immunohistochemistry. Tissues were processed using standard methods. Immunochemistry was performed using Dako EnVision+System peroxidase (DAB; Dako Corporation, Carpinteria, CA) according to the manufacturer's instructions.

Statistics. Unless stated otherwise, data are presented as means ± standard deviations (SD) and are representative of at least three independent experiments. Statistical significance was calculated using Student's *t* test.

RESULTS

Fumarase deficiency protects cells from apoptotic death. The response to apoptotic stimuli was studied in fumarase-defective human fibroblasts and renal cells (Fig. 1). FH-defective fibroblasts had been derived previously from the skin of patients suffering from fumaric aciduria (2). A mutant FH protein is expressed in these cells (Fig. 1A) and has severely reduced enzymatic activity (2, 34). FH-defective human renal cells were generated by expressing *FH*-specific shRNA by means of an LV in either RPTEC in primary culture (Fig. 1C) or HK-2 cells (Fig. 1E), which are RPTEC immortalized by E6/E7 expression (49). In both RPTEC and HK-2 cells, the LV allowed the random integration and expression of shRNAs in the majority of cells and thus effected a stable and long-term down modulation of FH (Fig. 1C and E). Fumarase knockdown resulted in reduced enzymatic activity, down to a residual activity of 7% of that measured in wild-type cells and comparable to that measured in FH-defective human fibroblasts, which carry a homozygous *FH* deletion (34). In all experiments where FH-specific interfering RNA was used, we utilized cells transduced with an LV carrying a scrambled shRNA sequence as a control. In addition, in FH-defective cells, FH activity was rescued (Fig. 1A and E) by the stable expression, driven by LV, of a human FH cDNA carrying eight silent mutations which rendered the corresponding mRNA unaffected by interference.

Survival of all FH-defective cells was tested after treatment with different stimuli inducing cell death. It is noteworthy that gene silencing driven by LV allows the study of bulk unselected cell populations, on the one hand, but on the other hand results in levels of FH silencing that vary from cell to cell depending on the number of integrated shRNA copies. Furthermore, cell synchronization was avoided because it involves cell exposure to a low serum concentration. Nevertheless, it was possible to demonstrate that human cells in primary cultures were protected from death when FH was knocked down (Fig. 1). FH deficiency resulted in protection from death of both FH-defective fibroblasts (Fig. 1B) and renal cells (Fig. 1D and F). Rescue of wild-type FH expression reversed this cell protection from death.

Next, we investigated whether FH-defective cells were protected from cell death mediated by apoptosis, as resistance to apoptosis is a fundamental feature of cancer cells which allows cells to accumulate multiple genetic defects. Figure 1G and H show that FH deficiency impacts an apoptotic program, as annexin V binding to the plasma membrane was not followed by consistent intracellular caspase-3 cleavage and cell permeabilization to propidium iodide.

HIF is stabilized in fumarase-defective cells, but protection from apoptosis is a HIF-independent mechanism. It was dem-

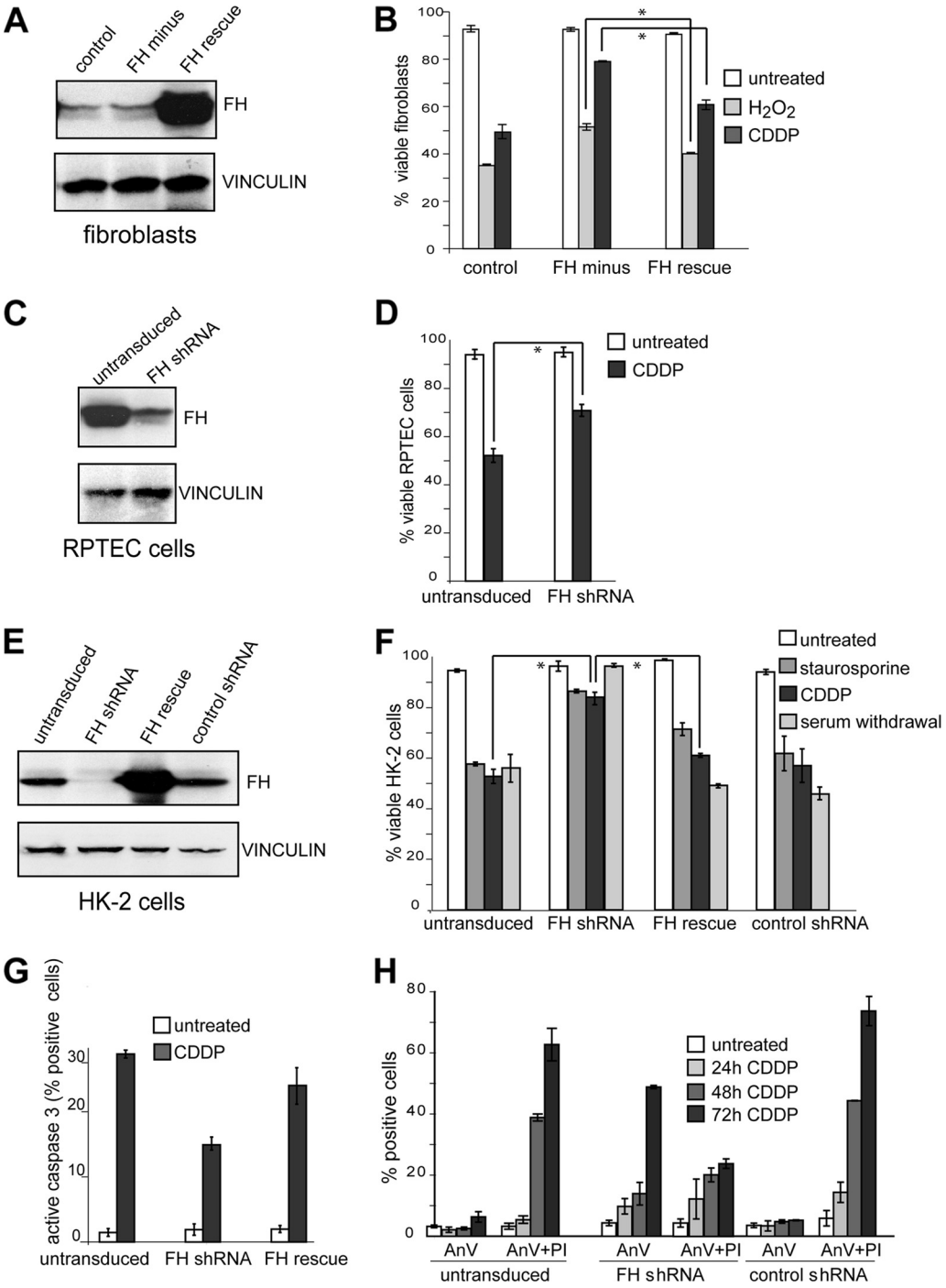

FIG 1 Fumarase-defective cells are protected from apoptosis. (A) FH-defective fibroblasts (FH minus) express an *FH* gene carrying homozygous missense mutations. In the same cells, transduction with a wild-type FH cDNA rescued the activity (FH rescue). Control fibroblasts are from a healthy individual. The blot was reprobed with a monoclonal antivinculin antibody to show equal loading. (B) FH-defective fibroblasts (FH minus) are protected from death induced by exposure to H_2O_2 and CDDP (1 mM and 20 μM, respectively) for 48 h, to which normal fibroblasts (control) and rescued fibroblasts are more susceptible. In this and the following apoptosis functional assays, healthy and treated cells were incubated with both annexin and propidium iodide, and cell viability was measured as the percentage of propidium iodide-negative cells. *, $P < 0.003$. (C) Decreased expression of the FH protein in primary cultured RPTEC transduced with a human FH-specific shRNA (FH shRNA). (D) Untransduced RPTEC are more susceptible to CDDP (20 μM for 48 h) than FH-defective RPTEC (FH shRNA). Cell viability was measured as described for panel B. *, $P < 0.006$. (E) Suppression of Fh protein expression in HK-2 cells transduced with FH-specific shRNA (FH shRNA). FH protein did not decrease in HK-2 cells transduced with a control shRNA. In FH-defective cells, FH expression was recovered after cell transduction with an shRNA-resistant FH cDNA (FH rescue). (F) FH knockdown in HK-2 cells resulted in cell protection from treatment with cisplatin (20 μM CDDP) and staurosporine (2.5 μM) for 48 h and from serum withdrawal for 7 days. Conversely, these treatments similarly killed untransduced cells and cells transduced with a control shRNA. In FH-defective cells, FH reexpression rescued cell susceptibility to cell death. Cell viability was measured as described for panel B. *, $P \leq 0.05$. (G) FH knockdown protected HK-2 cells from apoptosis, as they accumulated less activated caspase-3 after treatment with 20 μM CDDP for 48 h. (H) Time course of the apoptotic response of FH-defective cells to treatment with 20 μM CDDP. Cells which were in the early phase of apoptosis displayed a loss of plasma membrane asymmetry and were stained only with APC-labeled annexin V (AnV), which measures exposure of phosphatidylserine at the cell surface. Cells in the intermediate and late phases of apoptosis presented large plasma and nuclear membrane ruptures, which were revealed by simultaneous annexin V binding and propidium iodide (PI) staining.

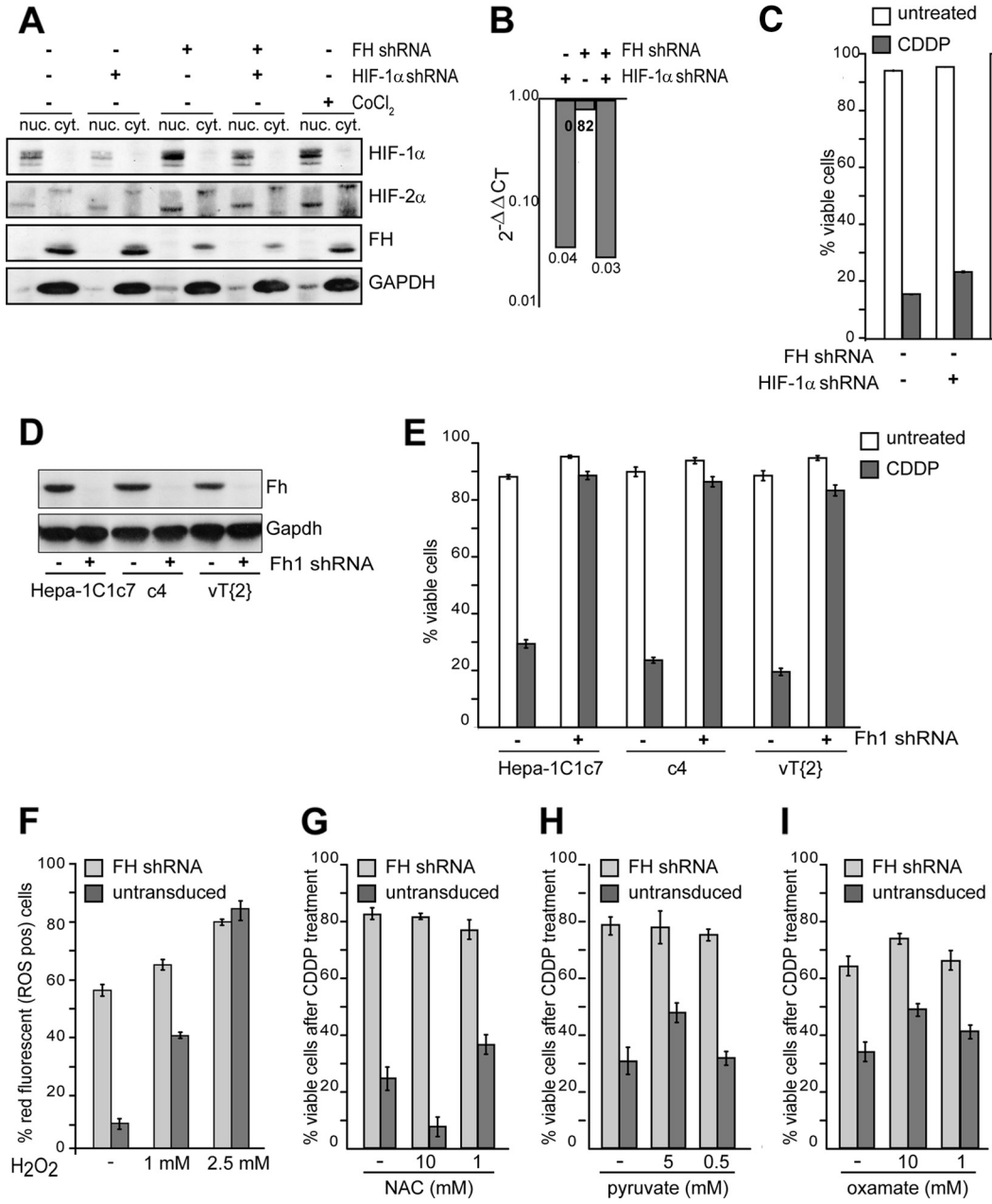

FIG 2 HIF-1α and HIF-2α are stabilized in FH-defective cells but are dispensable for cell protection from apoptosis. (A) Knocking down FH by interfering RNA (FH shRNA) in HK-2 cells resulted in nuclear (nuc.) but not cytoplasmic (cyt.) accumulation of HIF-1α and HIF-2α under normoxic conditions, comparable to that obtained by treating cells with 200 μM cobalt chloride ($CoCl_2$) for 24 h. To study the role of HIF-1α, the latter was down modulated by stable expression of a specific interfering shRNA (HIF-1α shRNA). The same Western blot was reprobed with a monoclonal GAPDH antibody to show equal loading. (B) HIF-1α down modulation by HIF-1α shRNA was also detectable at the mRNA level, as measured by quantitative real-time PCR. The mean fold change of HIF-1α gene expression was calculated using the following formula: $\Delta\Delta C_T = [(C_{T\,\text{HIF-1}\alpha} - C_{T\,\text{cyclophilin A}}$ for FH shRNA cells, HIF-1α shRNA cells, or HIF-1α shRNA and FH shRNA cells) − ($C_{T\,\text{HIF-1}\alpha} - C_{T\,\text{cyclophilin A}}$ for FH shRNA cells)]. (C) FH-defective HK-2 cells remained viable after treatment with 20 μM CDDP for 72 h and were not affected by the simultaneous down modulation of HIF-1α. Also, the response of FH-proficient HK-2 cells was not affected by HIF-1α knockdown. (D) Mouse *Fh1* was knocked down by means of stable expression of a specific interfering RNA (Fh shRNA) in the Hif-1β/Arnt-proficient mouse hepatoma Hepa-1C1c7 cell line; its mutant derivative subclone c4, which lacks a functional Hif-1β/Arnt protein; and a revertant clone of the c4 subclone, vT{2} cells, in which the functionality of the Arnt protein is restored by cDNA reexpression. Western blots were probed with a polyclonal anti-human FH antibody, which also labels the mouse protein, and with a monoclonal anti-mouse GAPDH antibody to show equal loading. (E) The aforementioned cells were protected from treatment with 20 μM CDDP for 72 h when FH was knocked down, irrespective of the functionality of Hif-1β/Arnt. (F) FH-defective HK-2 cells accumulated ROS even in the absence of added hydrogen peroxide (H_2O_2). ROS-positive cells were measured as the percentage of cells which accumulated the red fluorescent dye MitoSOX. (G to I) FH-defective HK-2 cells remained similarly viable when treated with 20 μM CDDP for 48 h in the presence of the indicated concentrations of either *N*-acetylcysteine (NAC) (G), sodium pyruvate (H), or the LDH inhibitor oxamate (I) or in the presence of vehicles used to dissolve the compounds (−).

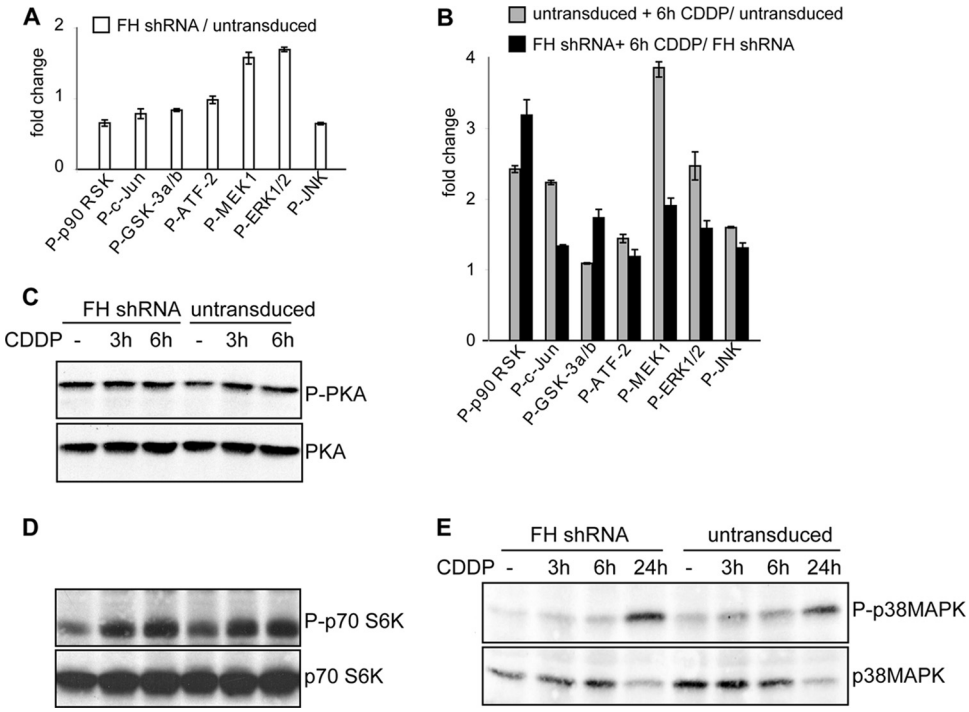

FIG 3 Survey of kinases activated in FH-defective cells. Phosphorylation of either kinase substrates or kinases themselves was studied as a surrogate marker of kinase activation, using the Bio-Plex phosphoprotein assay and Western blot analysis. HK-2 cells were exposed to 40 μM CDDP for the indicated times, which in most instances is known to activate survival kinases. (A) Phosphorylation was measured using the Bio-Plex phosphoprotein assay. The change in the phosphorylation level of each protein in FH-defective versus FH-proficient (untransduced) cells is shown. Bars show SD. (B) As described for panel A, phosphorylation of the same proteins was measured after CDDP treatment and is shown as the ratio of levels in treated versus untreated cells in FH-defective and FH-proficient (untransduced) cells. In panels C to E, Western blots of the phosphorylated forms of the indicated kinases are shown versus total protein expression. (C) PKA was similarly and modestly affected by CDDP in FH-defective and FH-proficient (untransduced) cells. (D) p70S6K was similarly activated by CDDP treatment in FH-defective and FH-proficient (untransduced) cells. (E) Increased phosphorylation of p38 MAPK was detected after 24 h of treatment with CDDP in both FH-defective and FH-proficient (untransduced) cells and was associated with decreased protein expression.

onstrated previously that in FH-defective cells and MCUL/HLRCC tumors (42, 44), the HIF-α subunits are stabilized and HIF-dependent transcription is induced. Using immunofluorescence, HIF-1α was found to have accumulated in the nuclei of the above-mentioned FH-defective human fibroblasts (P. Rustin, unpublished data). Accordingly, FH knockdown led to HIF-1α and HIF-2α nuclear accumulation in HK-2 cells under normoxic conditions (Fig. 2A).

Therefore, we first hypothesized that the survival advantage conferred by FH deficiency depends on HIF-1α subunit stabilization. To ascertain whether this was correct, FH-defective and FH-proficient HK-2 cells were transduced with LV carrying shRNAs specific for the human HIF-1α sequence. HIF-1α mRNA was decreased consistently in both FH-proficient and FH-defective cells (Fig. 2B), and the corresponding protein was down modulated concordantly (Fig. 2A). The apoptotic response was assayed in cells in which either FH or HIF-1α alone or both FH and HIF-1α were knocked down. Figure 2C shows evidence that FH-defective cells and FH-defective cells in which HIF-1α was down modulated were similarly protected from death. The same results were obtained after silencing of HIF-1α in cells by use of an LV carrying another HIF-1α-specific shRNA sequence (data not shown). This is also in agreement with our finding that Fh1 suppression makes Hif-1α knockout mouse embryo fibroblasts as resistant to apoptosis as wild-type MEFs (6). These data show that the protection from apoptosis due to FH knockdown is independent of HIF-1α.

Alternatively, HIF-2α might be responsible for the apoptotic protection observed in FH-defective cells, as HIF-1α and HIF-2α stimulate the expression of overlapping as well as unique transcriptional targets and their induction can have distinct biological effects (13). The HIF-2α protein, as well as HIF-1α, dimerizes with HIF-1β, also known as an aryl hydrocarbon receptor nuclear translocator (ARNT), to bind DNA and to activate transcription. In order to determine the role, if any, of the HIF-2α pathway in FH-defective cells, we used mouse cells lacking functional Hif-1β/Arnt, which were transduced with LV to stably express a murine *Fh1*-specific shRNA (Fig. 2D). Figure 2E shows that all the Fh1-defective cells were protected from death, regardless of the functionality of the HIF-2α pathway, thus demonstrating that HIF-2α stabilization does not contribute to cell survival of FH-defective nontransformed cells. This finding further ruled out the role of HIF-1α in the survival of FH-defective cells.

It has been reported (55) that FH loss might result in the generation of ROS. In agreement, we found a 5-fold increase in ROS levels in FH-defective HK-2 cells (Fig. 2F). To determine whether the increase in ROS contributes to cell protection from apoptosis, the response of FH-defective HK-2 cells to apoptotic stimuli was assayed in cells grown in the presence of either *N*-acetylcysteine or pyruvate, both of which are antioxidants. Protection from apoptosis was unaffected (Fig. 2G and H). In addition, it has been shown that when FH is lost in transformed cells, HIF stabilization results in increased expression of LDH, which can mediate cell

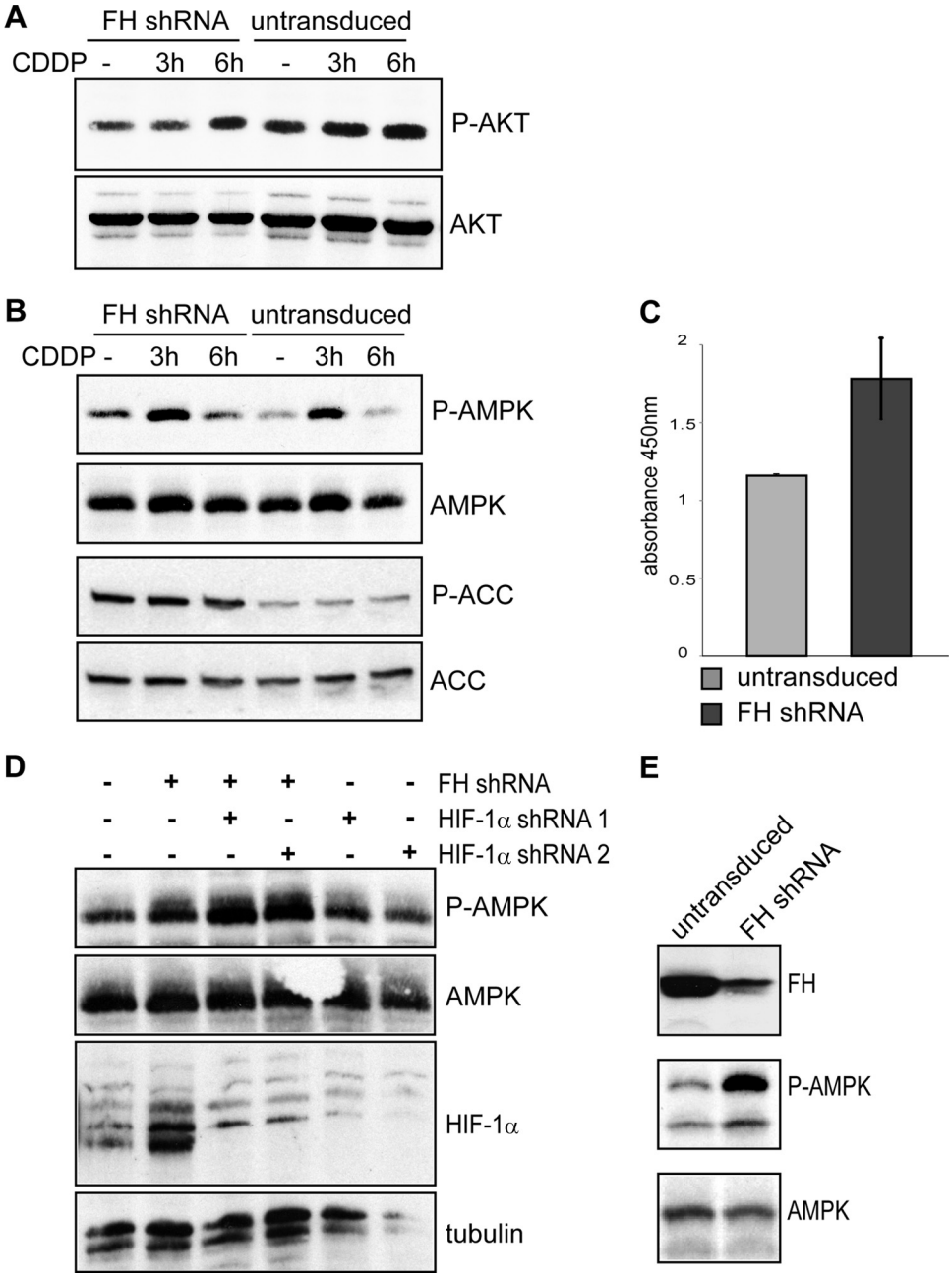

FIG 4 AMPK is constitutively activated in FH-defective normal kidney cells. (A) AKT was less phosphorylated at Ser473, indicating AKT activation, in FH-defective (FH shRNA) HK-2 cells than in control cells (untransduced). Phosphorylation was slightly increased after cell treatment with 40 μM CDDP. (B) In FH-defective (FH shRNA) HK-2 cells, AMPK was constitutively more phosphorylated at Thr172, which is marker of AMPK activation, and further activated by CDDP treatment. Activation of AMPK is also demonstrated by the increased phosphorylation of its specific substrate, ACC, labeled by an anti-P-ACC antibody. (C) A quantitative ELISA confirmed the increased phosphorylation of AMPK at Thr172 in FH-defective HK-2 cells compared to control cells. Results are presented as average absorbances ± SD for three independent experiments. In each experiment, the absolute absorbance at 450 nm was normalized to the protein concentration. (D) AMPK remained more phosphorylated in FH-defective HK-2 cells even when HIF-1α alone was down modulated by the specific shRNA. (E) FH down modulation (FH shRNA versus untransduced cells) also resulted in AMPK activation in primary cultured RPTEC.

protection from apoptosis (58). Thus, apoptosis was assayed in cells treated with the LDH inhibitor oxamate. Figure 2I shows that LDH inhibition did not hamper the survival of FH-defective cells.

Taken together, these data show that protection from apoptosis of FH-defective nontransformed kidney cells relies on a HIF-independent mechanism.

Fumarase knockdown protects cells from apoptosis by activating AMPK. Next, we investigated the molecular mechanism(s) underlying the survival advantage conferred by FH knockdown. We considered whether survival kinases were activated in response to apoptotic stimuli in FH-defective HK-2 cells. We carried out a survey with antibodies directed against

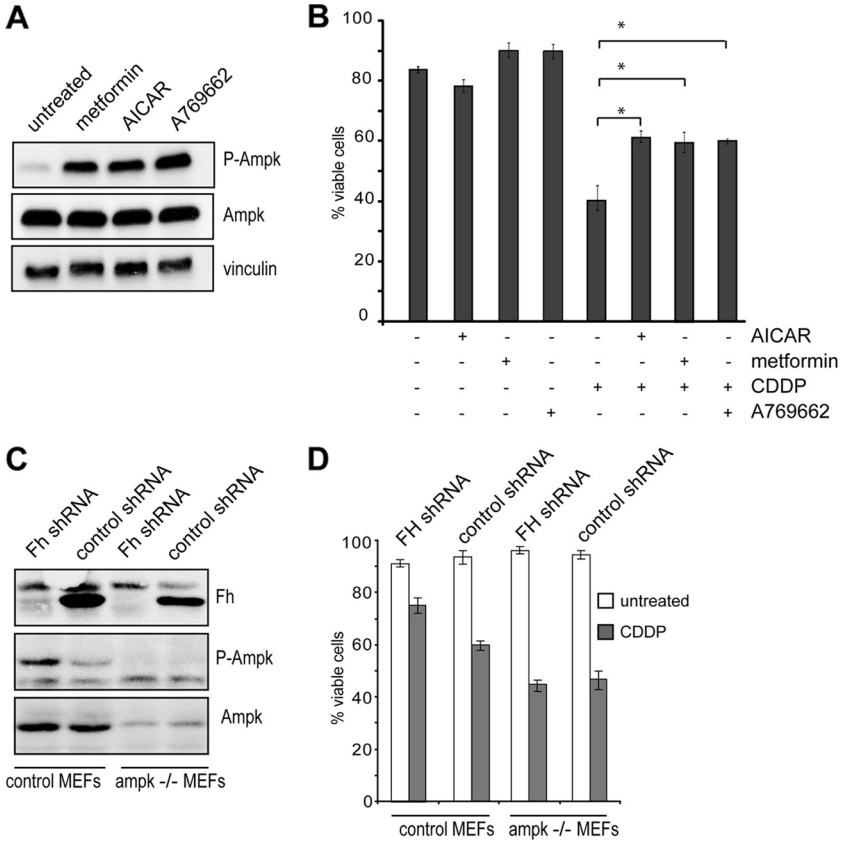

FIG 5 AMPK protects cells from apoptotic death and is necessary for the apoptosis protection mediated by FH suppression. (A) The treatment of FH-proficient HK-2 cells with AICAR (1 mM for 48 h), metformin (2 mM for 48 h), and A769662 (1 μM for 48 h), which are cell-permeating AMPK activators, resulted in increased AMPK phosphorylation at Thr172. (B) The apoptotic response to 20 μM CDDP for 48 h was analyzed, as in Fig. 1, in FH-proficient HK-2 cells. Either AICAR, metformin, or A769662 protected cells from apoptosis. Significance was calculated by comparing each triplicate of samples treated with an AMPK activator and CDDP to a triplicate of cells treated with CDDP alone. *, $P < 0.01$. (C) *fh1* suppression in control MEFs resulted in Ampk activation, which could not be seen in Ampk$^{-/-}$ MEFs. (D) CDDP treatment (40 μM for 48 h) affected control MEFs and Ampk$^{-/-}$ MEFs. Fh1 suppression protected control MEFs but not Ampk$^{-/-}$ MEFs against CDDP.

known kinase substrates and the phosphorylated forms of a number of candidate kinases (Fig. 3). Indeed, most kinases are themselves activated by phosphorylation at critical residues, and the phosphorylation status is a surrogate marker of their activation.

The mitogen-activated protein kinase (ERK1/2), the mitogen-activated protein kinase kinase 1 (MEK1), and the AMP-activated kinase (AMPK) were all constitutively more activated in untreated FH-defective cells than in untreated FH-proficient HK-2 cells (Fig. 3A and 4B), while the serine/threonine protein kinase AKT/PKB (Fig. 4A) and the ribosomal protein S6 kinase p90RSK (Fig. 3A) were less phosphorylated at residues marking activation. Cell treatment with an apoptotic stimulus did not increase the phosphorylation of MEK1 and ERK1/2 in FH-defective cells (Fig. 3B), while it slightly activated AKT and further increased AMPK activation (Fig. 4A, B, and C).

AMPK activation was also detected in FH-defective primary cultured kidney cells (Fig. 4E). Moreover, AMPK was activated by FH suppression in HK-2 cells in which HIF-1α was down modulated (Fig. 4D). This showed that HIF stabilization and AMPK activation were unrelated consequences of FH suppression.

We focused further analyses on AMPK, which is phosphorylated in FH-defective cells. Additionally, functional assays confirmed that AMPK activation is able to protect kidney cells from apoptosis. Activation was obtained using the AMPK activators AICAR, metformin, and A769662 (Fig. 5A and B). In the mirror experiment, the consistent simultaneous knockdown of both the α1 and α2 subunits of AMPK in both FH-depleted and control HK-2 cells resulted in cell death, irrespective of FH activity (data not shown).

To further substantiate the prosurvival role of AMPK in FH-defective cells, Fh1 was suppressed in Ampk α1/α2 double-knockout (Ampk$^{-/-}$) MEFs (29) (Fig. 5C). As shown in Fig. 5D, cisplatin treatment affected control MEFs and Ampk$^{-/-}$ MEFs. However, Fh1 suppression in control wild-type MEFs resulted in Ampk activation (Fig. 5C) and protected them, but not the Ampk$^{-/-}$ MEFs, from apoptosis (Fig. 5D), demonstrating the key role of Ampk in mediating the protective role of Fh1 suppression.

Activated kinases regulate cell survival at different levels. Because we had demonstrated (Fig. 1) that caspase-3 cleavage was reduced in FH-defective cells treated with an apoptotic stimulus, we investigated the known pathways regulating apoptosis. For HK-2 cells, we ruled out the role of p53, as these cells are immortalized by overexpression of the human papillomavirus E6/E7 oncoprotein, which downregulates p53 (49). We then studied members of the BCL2 family, a group of homologous proteins with

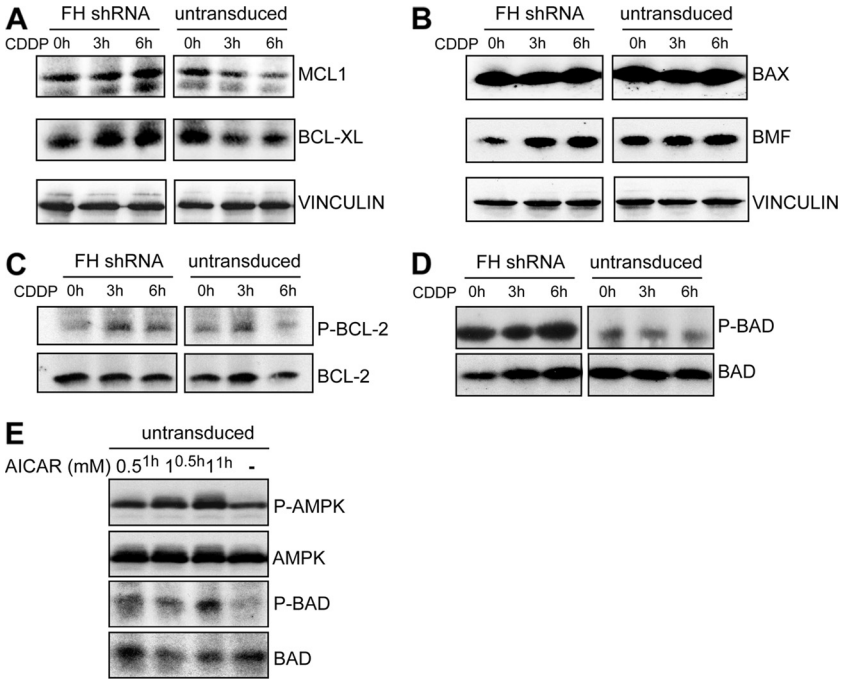

FIG 6 Study of Bcl-2 family members in FH-defective cells. Pro- and antiapoptotic activities of Bcl-2 family members are regulated at either the transcriptional or posttranscriptional level. Thus, expression (A and B) and phosphorylation (C and D) of a number of them were studied by Western blot analysis of FH-defective (FH shRNA) and FH-proficient (untransduced) HK-2 cells before and after treatment with 40 μM CDDP for the indicated times. (A) After treatment, both the prosurvival proteins MCL-1 and BCL-X_L were less decreased in FH-defective than in FH-proficient cells. (B) Expression of the proapoptotic proteins BMF and BAX was similarly induced by CDDP. (C) BCL-2 was comparably phosphorylated after treatment with CDDP in FH-defective and FH-proficient cells. (D) Conversely, the phosphorylation of BAD was higher in FH-defective HK-2 cells than in FH-proficient cells and was not modified by CDDP treatment. All blots were reprobed with either antibody against the total protein or a monoclonal vinculin antibody to show equal loading. (E) Treatment of FH-proficient HK-2 cells (untransduced) with AICAR, a cell-permeating AMPK activator, resulted in increased AMPK and BAD phosphorylation.

either pro- or antiapoptotic effects (3, 59), which initiate cell death at the mitochondrial level. We evaluated changes in the expression and phosphorylation of the following proteins in FH-defective HK-2 cells: the antiapoptotic proteins BCL2, BCL-X_L, and MCL1 and the proapoptotic proteins BAX, BAK, BAD, BIK/NBK, BIM/BOD, and BMF. Some data are shown in Fig. 6. We found that members of the BCL2 family are affected by FH suppression. The antiapoptotic MCL-1 and BCL-X_L proteins were increased rather than decreased by the apoptotic stimulus (Fig. 6A). Despite AMPK activation, we did not find increased expression of BIM (data not shown), which has been associated with excitotoxicity in neurons (4). BMF, described as the proapoptotic effector of AMPK activation in pancreatic beta cells (26), was even slightly upregulated by CDDP (Fig. 6B). Quantitative PCR analysis showed that MCL1 and BMF regulation occurred at the protein level (data not shown).

We observed that BAD, which is a proapoptotic protein, was regulated very differently in FH-defective cells and control cells (Fig. 6D): BAD was constitutively more phosphorylated and was not affected by an apoptotic stimulus in FH-deficient cells. A connection between AMPK activation and BAD phosphorylation has already been reported (9, 25, 45). In agreement, treatment of kidney cells with the AMPK activator AICAR resulted in increased BAD phosphorylation (Fig. 6E).

It is known that phosphorylation functionally impairs the proapoptotic activity of BAD. Thus, we investigated whether loss of BAD function impacts kidney cell survival. We silenced BAD expression in both FH-proficient and FH-defective HK-2 cells by using a human BAD-specific shRNA and the relevant control shRNA (50). Figure 7 shows that the resulting decrease in BAD expression made FH-proficient and FH-defective cells equally protected from apoptotic death.

Altogether, these data show, surprisingly, that the energy sensor AMPK, which is inactivated in several tumor types, is activated rather than inhibited after the loss of a mitochondrial tumor suppressor gene. AMPK activation affects members of the BCL2 family, which regulate the apoptosis machinery at the mitochondrial level.

AMPK is activated by fumarate accumulation in fumarase-defective cells. To assess whether AMPK might play a role in tumorigenesis initiated by loss of the FH tumor suppressor gene, we examined renal cysts from mice with targeted deletion of the *Fh1* gene (44). We observed an accumulation of the phosphorylated forms of AMPK and its specific substrate, acetyl coenzyme A carboxylase (ACC), in the epithelium lining the cysts (Fig. 8A, B, D, and E), which we have previously shown to be *Fh1*-null (44). Phospho-AMPK was also detected in 5/6 kidney cancers from HLRCC patients (Fig. 8G, H, J, and K).

To investigate the mechanism of AMPK activation after FH suppression, we measured the ADP:ATP ratio, as a relative loss of ATP triggers AMPK activation. As expected, ATP production was lower in FH-defective kidney cells than in control cells (Fig. 9A). However, reversion of the energetic impairment did not abolish AMPK phosphorylation. This was shown by studying MEFs isolated from mice bearing a conditionally inactivated *Fh1* allele ($Fh1^{-/-}$ MEFs). In $Fh1^{-/-}$ MEFs, Ampk was activated (constitu-

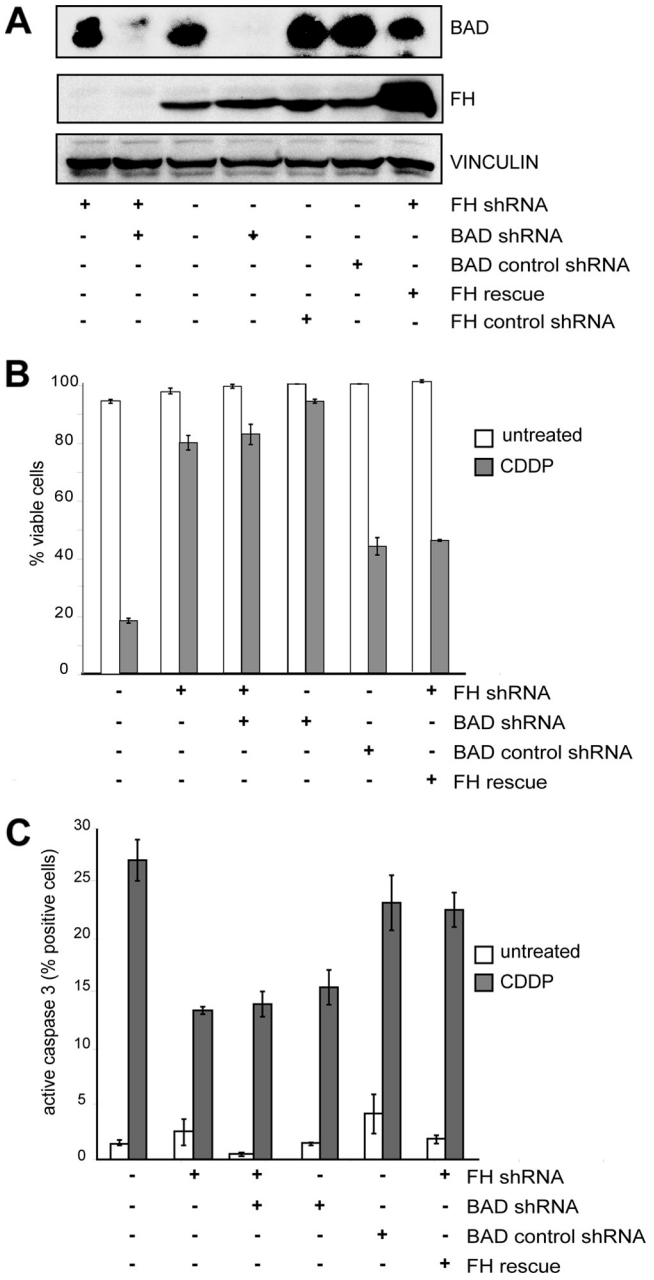

FIG 7 BAD is vital for protection of renal cells from apoptosis. (A) BAD expression was knocked down in HK-2 cells by stably transducing cells with a BAD-specific shRNA. Cells were also transduced to express the other indicated shRNA (FH specific or FH control) and with the FH cDNA (FH rescue). As a control for BAD-specific shRNA, cells were transduced with a scrambled BAD shRNA. (B) HK-2 cells in which either FH or BAD was down modulated remained similarly viable after treatment with 20 μM CDDP for 72 h. (C) Both BAD and FH knockdown protected HK-2 cells from an apoptotic death, as they similarly accumulated less activated caspase-3 after treatment with 20 μM CDDP for 48 h.

tively phosphorylated) (Fig. 9B and C). In *Fh1*$^{-/-}$ MEFs after the reexpression of a full-length human FH cDNA (39), fumarate accumulation was fully corrected and oxygen consumption and ATP levels were restored to normal (39). In these cells, Ampk activation was greatly diminished as a consequence (Fig. 9B). We then examined the effects of expressing an FH cDNA that lacks the mitochondrial targeting sequence (FHΔMTS) and is thus confined to the cytosol (Fig. 9B). Expression of FHΔMTS does not restore respiration and ATP loss but still lowers fumarate accumulation (39). In these cells, activated Ampk was still greatly diminished. Glucose supplementation of the culture medium of *Fh1*$^{-/-}$ MEFs did not lower AMPK activation; this was further activated, as expected, in cells growing in medium with a low concentration of glucose (Fig. 9D). These data suggested that fumarate accumulation, not defective respiration and subsequent energy deficiency, was responsible for AMPK activation. The data also confirmed that AMPK activation was not due to a change in the ADP:ATP ratio, as evidenced in cells where only the cytosolic Fh1 expression was restored (39; data not shown).

Fumarate is a potent inhibitor of some 2-oxoglutarate-dependent oxygenases (43). Therefore, we questioned whether AMPK activation in FH-deficient cells may be due to fumarate-mediated competitive inhibition of an oxygenase. To address this, we treated Fh1$^{-/-}$ MEFs (Fig. 9B) with cell-permeating 2-oxoglutarate. This has been shown previously to restore impaired HIF hydroxylation (36), including that in Fh1-deficent MEFs (39). Remarkably, AMPK activation was unaffected after treatment with 2-oxoglutarate and therefore is probably independent of oxygenase activity (Fig. 9B). These data suggest that AMPK activation in fumarase-defective cells is due to the accumulation of fumarate and are therefore indicative of a mechanism specific to fumarase deficiency and not due to the energetic impairment.

Another potential mechanism linking fumarate with AMPK activation is the involvement of G-protein-coupled receptors (GPCRs) (22). Among the hundreds of GPCRs encoded in the human genome (10), some have been identified which are activated by TCA cycle intermediates (18), including the succinate receptor (46). Since fumarate and succinate accumulate in FH-defective cells (42), we questioned whether fumarate, succinate, or both could activate AMPK through a receptor-mediated mechanism. Cells were exposed to monoethyl fumarate, diethylsuccinate, and exogenous succinate, with the latter being non-cell permeating. Both cell-permeating and -nonpermeating metabolites elicited ERK1/2 and AMPK activation in a 5- to 15-min time course and in temporal order (Fig. 9E and F).

In summary, these data show that the activation of AMPK observed in fumarase-defective cells is due to the accumulation of fumarate, and possibly also succinate, but not to energetic impairment or altered metabolic signaling. The kinetics of ERK1/2 and AMPK activation after acute exposure of kidney cells to TCA metabolites suggests that kinase activation might be due to GPCR activation.

DISCUSSION

Here we show that by avoiding death by apoptosis, cells defective in FH display a survival advantage which might contribute directly to tumorigenesis and that this property relies on activation of the energy sensor AMPK and is independent of the HIF pathway.

In agreement with previous reports (42, 51), we found that FH loss in normal kidney cells leads to both HIF-1α and HIF-2α accumulation but that these factors are not required for protection from apoptosis in this context. These data confirm our previous observation that Fh1 suppression makes Hif-1α knockout MEFs as resistant to apoptosis as wild-type MEFs (6). Moreover, a mouse model recently provided genetic evidence that Fh1-associated cyst formation is Hif independent (1). It is likely, however,

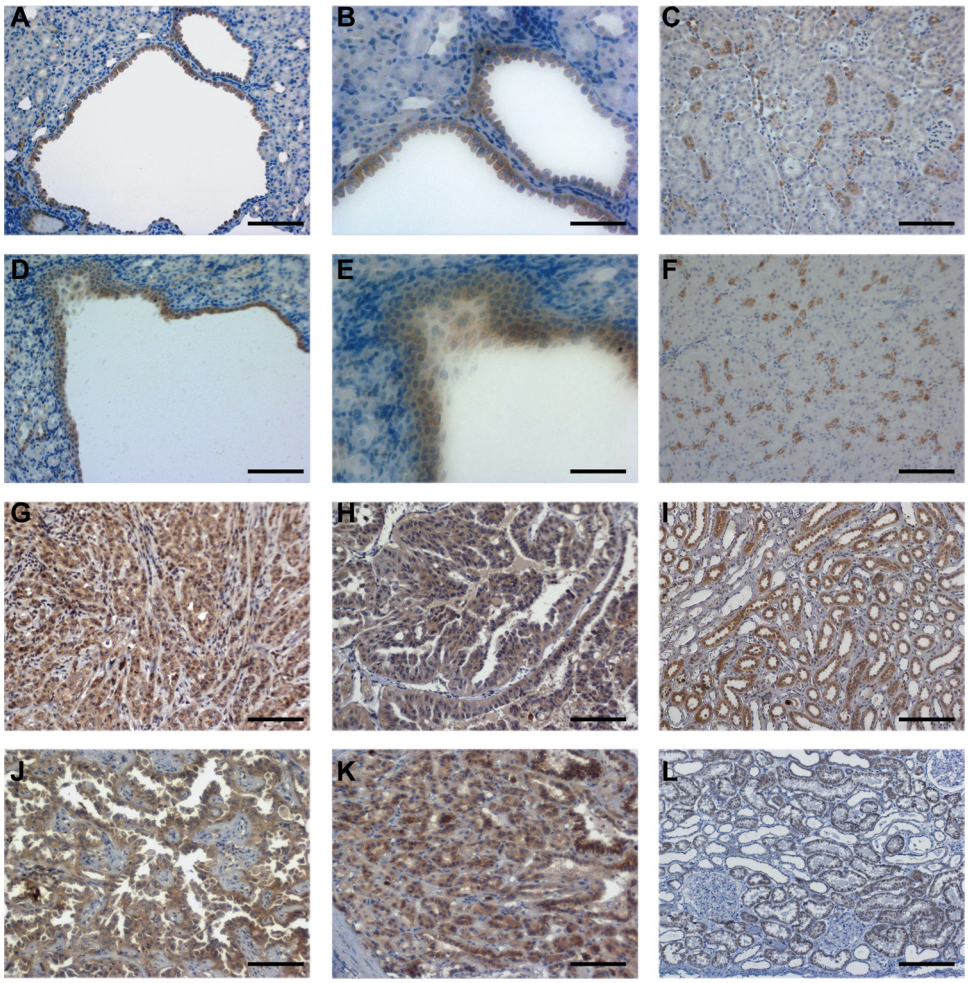

FIG 8 AMPK is activated in murine cysts and human papillary kidney tumors which have lost FH activity. (A and B) Phosphorylated, i.e., activated, P-Ampk was detected in epithelial cells lining mouse renal cysts from mice with an *fh1* targeted deletion, using anti-P-Ampk antibodies for immunohistochemistry. (C) In the mouse kidney, P-Ampk was detected, as expected, mainly in collecting ducts. (D to F) The phosphorylated form of ACC, a known Ampk substrate, was similarly distributed in both mouse renal cysts (D and E) and the mouse control kidney (F). The phosphorylated form of AMPK was detected in type II papillary renal cell carcinomas from HLRCC patients (G, H, J, and K) and in the collecting ducts of normal renal tissues (I and L). Bars, 50 μm (all panels but B and E) or 100 μm (B and E).

that HIF-1α and HIF-2α contribute to FH-defective cell survival *in vivo*, as they regulate the expression of antiapoptotic and proapoptotic genes and, in several instances, protect cells from death.

We found that AMPK is phosphorylated at threonine 172, i.e., activated, in normal cells in which FH activity is downregulated and the cells are protected from death. Moreover, FH suppression fails to protect normal kidney cells and fibroblasts devoid of AMPK activity. In mirror experiments, AMPK activation in normal kidney cells resulted in cell protection from death. Since AMPK was activated in these cells by AICAR, metformin, and A769662, which work through different mechanisms (17), we are confident that the results are indeed due to AMPK activation. Interestingly, we found that the phosphorylation (an indicator of activation) of AKT is reduced in FH-defective cells; this might contribute to AMPK activation, as it has been demonstrated that AKT inhibits AMPK activation and the associated phosphorylation at threonine 172 by phosphorylating the inhibitory threonine 485 of AMPK (38).

AMPK plays an antiapoptotic role under other physiological and pathological conditions: AMPK activation protects neurons from metabolic insults (28) and myocardial cells from injuries, both *in vitro* and *in vivo* (40, 48). In several instances, BCL2 family proteins have been implicated in protection mediated by AMPK activation (4, 9, 25, 26). We report here that among them, BAD is constitutively phosphorylated in FH-defective cells. Phosphorylation of BAD impairs its antiapoptotic role at the mitochondrial level, and several kinases which signal cell survival are known to regulate BAD phosphorylation (5). Also, activated AMPK has already been reported to protect cells by increasing the level of phosphorylated BAD, likely indirectly (9, 25, 45). We also found inhibition of c-Jun N-terminal kinase (JNK) in FH-defective cells (Fig. 3); this is interesting because it is known that BAD phosphorylation is also regulated by AMPK-dependent JNK inhibition (45).

Activation of AMPK in FH-defective cells is independent of HIF stabilization and is not due to ATP depletion, which we found in FH-defective cells both here and elsewhere (39), but to fumarate accumulation. However, it is not due to the metabolic signaling triggered by fumarate accumulation, which

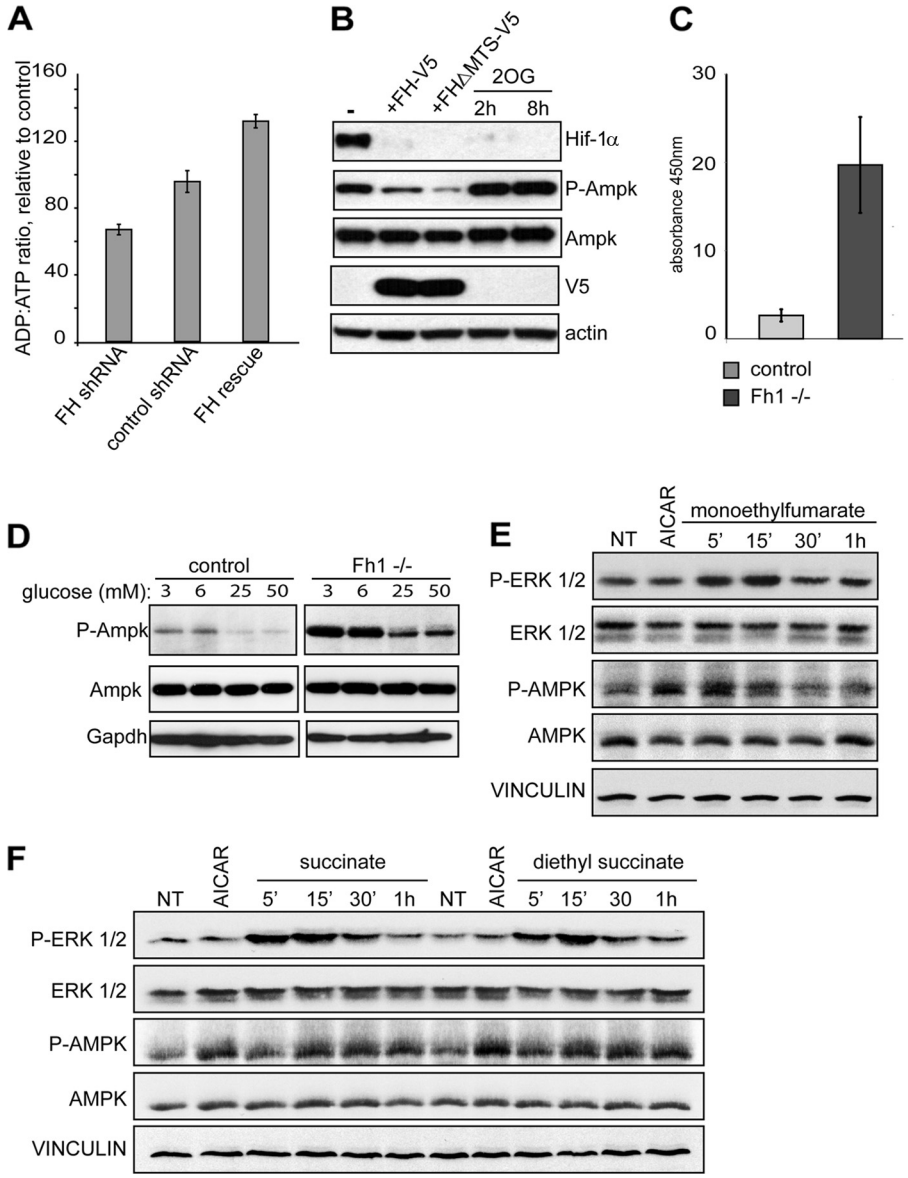

FIG 9 AMPK activation is due to fumarate accumulation in FH-defective cells. (A) The ADP:ATP ratio was decreased in FH-defective HK-2 cells. (B) In MEFs propagated from Fh1 knockout mice (Fh1$^{-/-}$ MEFs), Ampk was constitutively phosphorylated and Hif-1α was increased by stabilization. The expression of a V5-tagged cDNA encoding wild-type FH (FH-V5) abrogated Hif-1α stabilization and slightly reduced Ampk phosphorylation. The expression of the same V5-tagged cDNA devoid of the mitochondrial targeting sequence (FHΔMTS-V5) similarly abrogated Hif-1α stabilization and more strongly reduced Ampk phosphorylation. The treatment of Fh1$^{-/-}$ MEFs with 2-oxoglutarate (2OG), which reverts a blockade of 2-oxoglutarate-dependent oxygenases (2 mM for 2 and 8 h), abrogated Hif-1α stabilization but did not affect Ampk phosphorylation. (C) Quantitative ELISA confirmed that Fh1$^{-/-}$ MEFs displayed an increased phosphorylation of Ampk at Thr172 compared to wild-type MEFs (control). Results are presented as average absorbances ± SD for three independent experiments. In each experiment, the absolute absorbance at 450 nm was normalized to the protein concentration. (D) In Fh1-defective MEFs, Ampk is activated and activation is not suppressed by glucose supplementation of the medium to high concentrations (25 to 50 mM). Low concentrations of glucose (3 to 6 mM) activated Ampk in both control and Fh1-defective MEFs. (E) Treatment of FH-proficient HK-2 cells with monoethylfumarate (500 μM) for the indicated times resulted in increased ERK1/2 and AMPK phosphorylation. (F) Similarly, treatment of FH-proficient HK-2 cells with either succinate (200 μM) or diethyl succinate (200 μM) resulted in more ERK1/2 phosphorylation, i.e., activation, than that in untreated cells (NT); in temporal order, AMPK was phosphorylated to a level comparable to that obtained by treating cells with AICAR.

might lead to inhibition of the ferrous ion and 2-oxoglutarate-dependent oxygenases (33). This allowed unveiling of a new mechanism which might contribute to tumorigenesis due to FH tumor suppressor loss.

Succinate accumulates in FH-defective cells, in a manner similar to that of fumarate (42). We found that both fumarate and succinate trigger EKR1/2 and AMPK activation, with kinetics compatible with a receptor-mediated mechanism. This is not unexpected, as TCA metabolites can be excreted (30) and might activate GPCRs (18). Among the hundreds of GPCRs encoded in the human genome (10), a succinate receptor was found that is expressed distinctively in the kidney (46). Also, it has been shown that the succinate receptor activates ERK1/2 in kidney cells (47) and that a number of GPCRs might also activate AMPK (22),

independent of ERK1/2 activation. Intriguingly, each GPCR has a tissue-specific distribution (46), which might contribute to the understanding of tissue-specific tumorigenesis due to FH and succinate dehydrogenase (SDH) defects, which similarly stabilize HIF in all tissues (14).

AMPK is a highly conserved sensor of cellular energy status (16, 53) and suppresses cell growth and biosynthetic processes through the mammalian target-of-rapamycin pathway (16). Here we show that AMPK activation in nontransformed kidney cells, mouse kidney cysts, and kidney cancers of HLRCC patients does not result in inhibition of cell growth. In HK-2 cells, lack of inhibition might be due to p53 inactivation. In other cells, p27 phosphorylation and cytoplasmic accumulation might be hypothesized, as p27 might be phosphorylated by AMPK in both kidney cells and fibroblasts (27) and phosphorylation prevents p27 from translocating to the nucleus and inhibiting the cell cycle. The AMPK upstream activator is the protein product of the LKB1 tumor suppressor gene (54). Oncogenic mutations might actively dismantle the LKB1-AMPK axis (60). Such data highlight the role of AMPK as a member of tumor-suppressive pathways. We demonstrate here that, surprisingly, AMPK might play an "oncogenic" role in human cells. The activated form of AMPK accumulated not only *in vitro*, in FH-defective renal cells and $Fh1^{-/-}$ MEFs, but also *in vivo*, in mouse cysts of *Fh1*-null mice and in a number of papillary renal cell carcinoma samples from HLRCC patients. These data show that AMPK activation not only might be an early and possibly transitory event in FH-driven tumorigenesis but also might sustain cell protection from death in established cancer. The latter might appear in contrast to the results reported by Tong et al. (57), who showed that AMPK was suppressed in spontaneously immortalized cell lines from papillary renal cell carcinomas of HLRCC patients. They also showed three tumor samples negative for AMPK staining. Because we also found one negative sample, we could infer that stringent conditions might drive selection of more aggressive cancer cells, which likely require AMPK suppression to surmount accumulation of genetic defects.

These findings, besides highlighting a new mechanism for FH loss in tumorigenesis and a novel role for AMPK in both normal and transformed cells, are important in considering AMPK activation as a therapeutic strategy against cancer (16, 41). Targeting AMPK is immediately feasible, as metformin is approved for the therapy of diabetes. Preclinical (20, 21) and epidemiological (24, 31, 32) studies have prompted clinical trials (12, 15) to evaluate the effects of metformin on the treatment or prevention of human cancer. Regrettably, we show here that AMPK activation not only might be ineffective but also might be harmful when tumors present with a particular genetic profile, such as inactivation of FH, p53, and cell cycle inhibitors or expression of AMPK. This suggests that the molecular profile of every tumor should be evaluated before reactivating treatment and reinforces the need to personalize each patient's treatment on the basis of the genetic and molecular characteristics of that patient's tumor.

ACKNOWLEDGMENTS

We are grateful to G. Kulik (Wake Forest University Health Sciences, Winston-Salem, NC) for BAD-specific shRNA and relevant controls and to B. Viollet (Institut Cochin INSERM U1016, CNRS UMR 8104, Université Paris Descartes Department of Endocrinology, Metabolism and Cancer, Paris, France) for Ampk α1/α2 double-knockout mouse embryo fibroblasts and the relevant control fibroblasts. The technical help of Enzo De Sio and Raffaella Albano is acknowledged.

This work was supported by grants from the Italian Association for Cancer Research (AIRC) and from Regione Piemonte to M.F.D.R. P.J.P. is the recipient of a Beit Memorial Fellowship funded by the Wellcome Trust (grant WT091112MA).

We have no conflicts of interest to disclose.

REFERENCES

1. **Adam J, et al.** 2011. Renal cyst formation in Fh1-deficient mice is independent of the Hif/Phd pathway: roles for fumarate in KEAP1 succination and Nrf2 signaling. Cancer Cell **20**:524–537.
2. **Bourgeron T, et al.** 1994. Mutation of the fumarase gene in two siblings with progressive encephalopathy and fumarase deficiency. J. Clin. Invest. **93**:2514–2518.
3. **Chao DT, Korsmeyer SJ.** 1998. BCL-2 family: regulators of cell death. Annu. Rev. Immunol. **16**:395–419.
4. **Concannon CG, et al.** 2010. AMP kinase-mediated activation of the BH3-only protein Bim couples energy depletion to stress-induced apoptosis. J. Cell Biol. **189**:83–94.
5. **Cory S, Adams JM.** 2002. The Bcl2 family: regulators of the cellular life-or-death switch. Nat. Rev. Cancer **2**:647–656.
6. **Costa B, et al.** 2010. Fumarase tumor suppressor gene and MET oncogene cooperate in upholding transformation and tumorigenesis. FASEB J. **24**: 2680–2688.
7. **DeBerardinis RJ, Lum JJ, Hatzivassiliou G, Thompson CB.** 2008. The biology of cancer: metabolic reprogramming fuels cell growth and proliferation. Cell Metab. **7**:11–20.
8. **Denko NC.** 2008. Hypoxia, HIF1 and glucose metabolism in the solid tumour. Nat. Rev. Cancer **8**:705–713.
9. **Depre C, et al.** 2006. H11 kinase prevents myocardial infarction by preemptive preconditioning of the heart. Circ. Res. **98**:280–288.
10. **Fredriksson R, Schioth HB.** 2005. The repertoire of G-protein-coupled receptors in fully sequenced genomes. Mol. Pharmacol. **67**:1414–1425.
11. **Frezza C, et al.** 2011. Haem oxygenase is synthetically lethal with the tumour suppressor fumarate hydratase. Nature **477**:225–228.
12. **Goodwin PJ, Ligibel JA, Stambolic V.** 2009. Metformin in breast cancer: time for action. J. Clin. Oncol. **27**:3271–3273.
13. **Gordan JD, Simon MC.** 2007. Hypoxia-inducible factors: central regulators of the tumor phenotype. Curr. Opin. Genet. Dev. **17**:71–77.
14. **Gottlieb E, Tomlinson IP.** 2005. Mitochondrial tumour suppressors: a genetic and biochemical update. Nat. Rev. Cancer **5**:857–866.
15. **Hadad S, et al.** 2011. Evidence for biological effects of metformin in operable breast cancer: a pre-operative, window-of-opportunity, randomized trial. Breast Cancer Res. Treat. **128**:783–794.
16. **Hardie DG.** 2007. AMP-activated/SNF1 protein kinases: conserved guardians of cellular energy. Nat. Rev. Mol. Cell. Biol. **8**:774–785.
17. **Hawley SA, et al.** 2010. Use of cells expressing gamma subunit variants to identify diverse mechanisms of AMPK activation. Cell Metab. **11**:554–565.
18. **He W, et al.** 2004. Citric acid cycle intermediates as ligands for orphan G-protein-coupled receptors. Nature **429**:188–193.
19. **Hewitson KS, et al.** 2007. Structural and mechanistic studies on the inhibition of the hypoxia-inducible transcription factor hydroxylases by tricarboxylic acid cycle intermediates. J. Biol. Chem. **282**:3293–3301.
20. **Hirsch HA, et al.** 2010. A transcriptional signature and common gene networks link cancer with lipid metabolism and diverse human diseases. Cancer Cell **17**:348–361.
21. **Huang X, et al.** 2008. Important role of the LKB1-AMPK pathway in suppressing tumorigenesis in PTEN-deficient mice. Biochem. J. **412**:211–221.
22. **Hutchinson DS, Summers RJ, Bengtsson T.** 2008. Regulation of AMP-activated protein kinase activity by G-protein coupled receptors: potential utility in treatment of diabetes and heart disease. Pharmacol. Ther. **119**: 291–310.
23. **Isaacs JS, et al.** 2005. HIF overexpression correlates with biallelic loss of fumarate hydratase in renal cancer: novel role of fumarate in regulation of HIF stability. Cancer Cell **8**:143–153.
24. **Jiralerspong S, et al.** 2009. Metformin and pathologic complete responses to neoadjuvant chemotherapy in diabetic patients with breast cancer. J. Clin. Oncol. **27**:3297–3302.
25. **Kewalramani G, et al.** 2009. AMP-activated protein kinase confers pro-

tection against TNF-alpha-induced cardiac cell death. Cardiovasc. Res. **84**:42–53.
26. **Kilbride SM, et al.** 2010. AMP-activated protein kinase mediates apoptosis in response to bioenergetic stress through activation of the pro-apoptotic Bcl-2 homology domain-3-only protein BMF. J. Biol. Chem. **285**:36199–36206.
27. **Kossatz U, et al.** 2006. C-terminal phosphorylation controls the stability and function of p27kip1. EMBO J. **25**:5159–5170.
28. **Kuramoto N, et al.** 2007. Phospho-dependent functional modulation of GABA(B) receptors by the metabolic sensor AMP-dependent protein kinase. Neuron **53**:233–247.
29. **Laderoute KR, et al.** 2006. 5′-AMP-activated protein kinase (AMPK) is induced by low-oxygen and glucose deprivation conditions found in solid-tumor microenvironments. Mol. Cell. Biol. **26**:5336–5347.
30. **Lewis GD, et al.** 2010. Metabolic signatures of exercise in human plasma. Sci. Transl. Med. **2**:33ra37.
31. **Li D, Yeung SC, Hassan MM, Konopleva M, Abbruzzese JL.** 2009. Antidiabetic therapies affect risk of pancreatic cancer. Gastroenterology **137**:482–488.
32. **Libby G, et al.** 2009. New users of metformin are at low risk of incident cancer: a cohort study among people with type 2 diabetes. Diabetes Care **32**:1620–1625.
33. **Loenarz C, Schofield CJ.** 2008. Expanding chemical biology of 2-oxoglutarate oxygenases. Nat. Chem. Biol. **4**:152–156.
34. **Lorenzato A, et al.** 2008. A cancer-predisposing "hot spot" mutation of the fumarase gene creates a dominant negative protein. Int. J. Cancer **122**:947–951.
35. **Luo J, Solimini NL, Elledge SJ.** 2009. Principles of cancer therapy: oncogene and non-oncogene addiction. Cell **136**:823–837.
36. **MacKenzie ED, et al.** 2007. Cell-permeating alpha-ketoglutarate derivatives alleviate pseudohypoxia in succinate dehydrogenase-deficient cells. Mol. Cell. Biol. **27**:3282–3289.
37. **Majmundar AJ, Wong WJ, Simon MC.** 2010. Hypoxia-inducible factors and the response to hypoxic stress. Mol. Cell **40**:294–309.
38. **Mankouri J, et al.** 2010. Enhanced hepatitis C virus genome replication and lipid accumulation mediated by inhibition of AMP-activated protein kinase. Proc. Natl. Acad. Sci. U. S. A. **107**:11549–11554.
39. **O'Flaherty L, et al.** 2010. Dysregulation of hypoxia pathways in fumarate hydratase-deficient cells is independent of defective mitochondrial metabolism. Hum. Mol. Genet. **19**:3844–3851.
40. **Paiva MA, et al.** 2010. Transitory activation of AMPK at reperfusion protects the ischaemic-reperfused rat myocardium against infarction. Cardiovasc. Drugs Ther. **24**:25–32.
41. **Pollak M.** 2008. Insulin and insulin-like growth factor signalling in neoplasia. Nat. Rev. Cancer **8**:915–928.
42. **Pollard PJ, et al.** 2005. Accumulation of Krebs cycle intermediates and over-expression of HIF1alpha in tumours which result from germline FH and SDH mutations. Hum. Mol. Genet. **14**:2231–2239.
43. **Pollard PJ, Ratcliffe PJ.** 2009. Cancer. Puzzling patterns of predisposition. Science **324**:192–194.
44. **Pollard PJ, et al.** 2007. Targeted inactivation of fh1 causes proliferative renal cyst development and activation of the hypoxia pathway. Cancer Cell **11**:311–319.
45. **Qi D, et al.** 2009. Cardiac macrophage migration inhibitory factor inhibits JNK pathway activation and injury during ischemia/reperfusion. J. Clin. Invest. **119**:3807–3816.
46. **Regard JB, Sato IT, Coughlin SR.** 2008. Anatomical profiling of G protein-coupled receptor expression. Cell **135**:561–571.
47. **Robben JH, et al.** 2009. Localization of the succinate receptor in the distal nephron and its signaling in polarized MDCK cells. Kidney Int. **76**:1258–1267.
48. **Russell RR, 3rd, et al.** 2004. AMP-activated protein kinase mediates ischemic glucose uptake and prevents postischemic cardiac dysfunction, apoptosis, and injury. J. Clin. Invest. **114**:495–503.
49. **Ryan MJ, et al.** 1994. HK-2: an immortalized proximal tubule epithelial cell line from normal adult human kidney. Kidney Int. **45**:48–57.
50. **Sastry KS, Smith AJ, Karpova Y, Datta SR, Kulik G.** 2006. Diverse antiapoptotic signaling pathways activated by vasoactive intestinal polypeptide, epidermal growth factor, and phosphatidylinositol 3-kinase in prostate cancer cells converge on BAD. J. Biol. Chem. **281**:20891–20901.
51. **Selak MA, et al.** 2005. Succinate links TCA cycle dysfunction to oncogenesis by inhibiting HIF-alpha prolyl hydroxylase. Cancer Cell **7**:77–85.
52. **Semenza GL.** 2003. Targeting HIF-1 for cancer therapy. Nat. Rev. Cancer **3**:721–732.
53. **Shackelford DB, Shaw RJ.** 2009. The LKB1-AMPK pathway: metabolism and growth control in tumour suppression. Nat. Rev. Cancer **9**:563–575.
54. **Shaw RJ, et al.** 2004. The tumor suppressor LKB1 kinase directly activates AMP-activated kinase and regulates apoptosis in response to energy stress. Proc. Natl. Acad. Sci. U. S. A. **101**:3329–3335.
55. **Sudarshan S, et al.** 2009. Fumarate hydratase deficiency in renal cancer induces glycolytic addiction and HIF-1alpha stabilization by glucose-dependent generation of reactive oxygen species. Mol. Cell. Biol. **29**:4080–4090.
56. **Tomlinson IP, et al.** 2002. Germline mutations in FH predispose to dominantly inherited uterine fibroids, skin leiomyomata and papillary renal cell cancer. Nat. Genet. **30**:406–410.
57. **Tong WH, et al.** 2011. The glycolytic shift in fumarate-hydratase-deficient kidney cancer lowers AMPK levels, increases anabolic propensities and lowers cellular iron levels. Cancer Cell **20**:315–327.
58. **Xie H, et al.** 2009. LDH-A inhibition, a therapeutic strategy for treatment of hereditary leiomyomatosis and renal cell cancer. Mol. Cancer Ther. **8**:626–635.
59. **Youle RJ, Strasser A.** 2008. The BCL-2 protein family: opposing activities that mediate cell death. Nat. Rev. Mol. Cell. Biol. **9**:47–59.
60. **Zheng B, et al.** 2009. Oncogenic B-RAF negatively regulates the tumor suppressor LKB1 to promote melanoma cell proliferation. Mol. Cell **33**:237–247.